Soliton mode-locked fiber laser based on topological insulator Bi_2Te_3 nanosheets at 2 μm

Ke Yin,[1,*] Bin Zhang,[1] Lei Li,[1] Tian Jiang,[1,2] Xuanfeng Zhou,[1] and Jing Hou[1,3]

[1]*College of Optoelectronic Science and Engineering, National University of Defense Technology, Changsha 410073, China*
[2]*e-mail: jiangtian198611@163.com*
[3]*e-mail: houjing25@sina.com*
**Corresponding author: cqyinke@126.com*

Received January 6, 2015; revised February 14, 2015; accepted February 23, 2015; posted February 24, 2015 (Doc. ID 231613); published April 9, 2015

We reported diverse soliton operations in a thulium/holmium-doped fiber laser by taking advantage of a tapered fiber-based topological insulator (TI) Bi_2Te_3 saturable absorber (SA). The SA had a nonsaturable loss of ~53.5% and a modulation depth of 9.8%. Stable fundamentally mode-locked solitons at 1909.5 nm with distinct Kelly sidebands on the output spectrum, a pulse repetition rate of 21.5 MHz, and a measured pulse width of 1.26 ps were observed in the work. By increasing the pump power, both bunched solitons with soliton number up to 15 and harmonically mode-locked solitons with harmonic order up to 10 were obtained. To our knowledge, this is the first report of both bunched solitons and harmonically mode-locked solitons in a fiber laser at 2 μm region incorporated with TIs. © 2015 Chinese Laser Press

OCIS codes: (060.5530) Pulse propagation and temporal solitons; (140.7090) Ultrafast lasers; (140.0140) Lasers and laser optics; (140.4050) Mode-locked lasers; (160.4330) Nonlinear optical materials.
http://dx.doi.org/10.1364/PRJ.3.000072

1. INTRODUCTION

Optical solitons, formed as a result of the interplay between dispersion and nonlinear effects in optical fibers, have attracted tremendous research interest since 1980s [1]. Technologically speaking, they play great roles in numerous areas like optical fiber communication, ultrafast optics, optical metrology, and so on. Solitons can be readily generated in optical fiber lasers with both active and passive mode-locking techniques [2,3]. Moreover, passive mode-locking techniques benefitting from either tangible saturable absorbers (SAs) or intra-cavity nonlinear effects are deemed as the better vehicle to obtain solitons in fiber lasers for their simplicity and good performance [4,5]. By choosing moderate conditions (with different kinds of SAs and gain fibers) in filter-free fiber resonators, optical solitons have been widely reported [6,7].

Very recently, topological insulators (TIs) as a two-dimensional material have attracted great attention due to their unique electronic and optical properties such as good thermal management, high nonlinear refraction index, and ultrafast relaxation time [8,9]. Ever since the first demonstration of optical SA-like behavior of TI Bi_2Te_3 at 1550 nm in 2012 [10], mode-locked fiber lasers with TI materials (including Bi_2Te_3 [11–13], Bi_2Se_3 [14], Sb_2Te_3 [15,16], and MoS_2 [17–20]) have been investigated. Most of these investigations focus on the ytterbium-doped fiber lasers at 1 μm [13,19,20] and erbium-doped fiber lasers at 1.5 μm [11,12,14–18], but at present reports of mode-locked fiber lasers at 2 μm incorporated with TI materials are still rare [21]. The energy gap of Bi_2Te_3 is ~0.3 eV, which corresponds to the absorbance ability of light with wavelengths shorter than 4.1 μm and the possibility of its application in mode-locked fiber lasers at the 2 μm wavelength region.

It is known that the 2 μm wavelength region covers various gas absorption lines (e.g., H_2O, CO, and CO_2) which may be useful in atmospheric sensing [22,23] and also it is deemed as the most promising pump band for wavelength conversion to the mid-infrared molecular fingerprint region [e.g., for $ZnGeP_2$-based optical parametric oscillator (OPO)] [24] and supercontinuum generation [25,26]). The ultra-wide gain spectrum of thulium or holmium-doped fibers at 2 μm makes them favorable to generate ultrafast mode-locked pulses. Advances of 2 μm mode-locked fiber lasers can be found in a recent review paper [27]. Therefore, demonstration of the TI-based SA to ultrafast fiber laser at the 2 μm region is still interesting and important such that needs to be further explored.

In this paper, we report our recent investigations on a soliton mode-locked fiber laser at 2 μm by adopting TI Bi_2Te_3 nanosheets. The TI-based SA was prepared by optically depositing high-quality Bi_2Te_3 nanosheets onto a piece of single-mode fiber (SMF) with cladding diameter tapered down to ~14 μm. Self-started fundamentally mode-locked soliton pulses with a measured 3 dB spectral width of 3.43 nm, a pulse repetition rate of 21.5 MHz, and a pulse with of 1.26 ps (after amplification) were recorded. Moreover, by adjusting the cavity polarization and increasing the whole gain, stable soliton bunches with soliton number up to 15 in a single bunch and over 10th-order harmonically mode-locked soliton pulses were realized.

2. EXPERIMENTAL SETUP

In a synthesis, a moderate thylene glycol was used to dissolve a stoichiometric ratio of bismuth chloride ($BiCl_3$) and sodium selenide (Na_2TeO_3) together with vigorous stirring. The mixture was transferred into an autoclave to obtain gray Bi_2Te_3

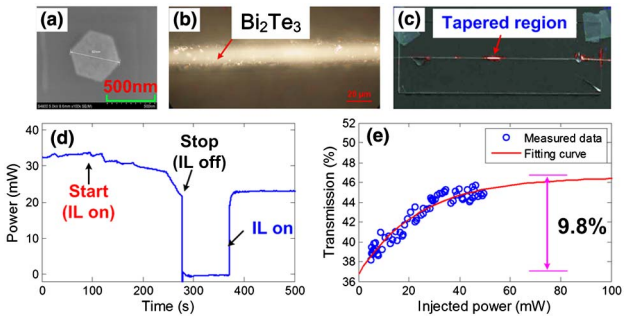

Fig. 1. (a) SEM photograph of the TI Bi_2Te_3 nanosheets; (b) microscope photo of the TI-based SA; (c) photo of the TI-based SA via visible light; (d) time-dependent depositing process; (e) nonlinear SA curve.

powder, then washed with distilled water and ethanol, and finally dried at 60°C in vacuum. The as-grown and washed powders had typical hexagonal morphologies with dimensions between 400 and 600 nm measured with a scanning electron microscope (SEM), as shown in Fig. 1(a). Their thickness was measured to be ~20 nm with an atomic force microscope. These powders were then dispersed in an ethanol solution with a concentration of ~100 μg/mL. The Bi_2Te_3 dispersion was optically deposited onto a piece of tapered SMF–28^{e+} (with cladding diameter tapered down to ~14 μm and tapered length of ~1 cm) to make the TI-based SA. The tapered fiber was placed on a quartz plate. A 976 nm fiber-coupled laser diode with 40 mW average output power was adopted as the illuminated light (IL), and the depositing process was monitored with a power meter. The deposition process took only ~170 s, then the IL was turned off. About 100 s later, the ethanol solution was completely evaporated. As the last step, the IL was turned on again to measure the loss of the TI-based SA.

Figure 1(b) shows a microscope photo of the tapered region of TI-based SA with a 1000-fold magnification. By coupling red light (632.8 nm) into the SA, the evanescent filed could be revealed as shown in Fig. 1(c). The time-dependent variation of monitored power during the depositing process is plotted in Fig. 1(d) showing that the TI-based SA had an insertion loss of ~2.4 dB at 976 nm. The saturable characteristics of the previously fabricated TI-based SA was also investigated by using a homemade mode-locked thulium-doped fiber laser which delivers ~3 ps laser pulses at 1960 nm with a repetition rate of 10.56 MHz. Figure 1(e) plots the measured peak-power-dependent transmission data of TI-based SA and the corresponding fitting curve. As can be seen, the modulation depth of TI-based SA is ~9.8% and the nonsaturable loss is ~53.5%.

The TI-based SA was incorporated into a ring cavity thulium/holmium-doped fiber laser (THDFL). Figure 2 depicts the experimental setup of the THDFL. The lasing gain at 2 μm was provided by a 2 m length of single-mode thulium/holmium-doped fiber (THDF) pumped by a 1570 nm continuous-wave fiber laser via a 1570/2000 nm wavelength division multiplexer (WDM). The single-mode THDF had a core/cladding diameter of 9/125 μm with a core numerical aperture of 0.15 and absorption coefficient of ~10 dB/m at 1550 nm. The other end of THDF was spliced to a polarization-independent isolator (ISO) to ensure the unidirectional propagation of

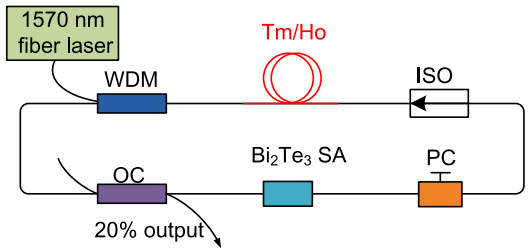

Fig. 2. Experimental setup of the passively mode-locked THDFL.

intra-cavity light. Between the TI-based SA and the ISO, a polarization controller (PC) was used to adjust the cavity polarization. The laser output was extracted from the 20% port of a fused fiber-optical coupler (OC).

The laser output were detected with an extended InGaAs photodetector (bandwidth 9 GHz) monitored on a digital oscilloscope (bandwidth 1.5 GHz). And a second harmonic generation based autocorrelator was used to measure the pulse width. A thulium-doped fiber amplifier (TDFA) was put before the autocorrelator in order to get high peak power of the output pulses to induce a detectable second harmonic signal. A grating based optical spectrum analyzer was used to measure the laser spectrum with a resolution of 0.05 nm. Other measuring equipment includes a thermal power meter, and a radio frequency (RF) spectrum analyzer (bandwidth 26.5 GHz).

3. EXPERIMENTAL RESULTS AND DISCUSSION

In the work, by increasing the pump power, amplified spontaneous emission (ASE) light and self-lasing with output spectrum peaked at ~1909 nm were observed first. Then we adjusted the intra-cavity polarization states by rotating the PC and increasing a little pump power to ~315 mW, stable fundamentally mode-locked soliton pulses could be readily observed.

The measured spectrum of the output soliton is depicted in Fig. 3(a), showing pairs of Kelly sidebands which located almost symmetrically with respect to the central wavelength (1909.5 nm) of the spectrum. The spectral dips as shown in

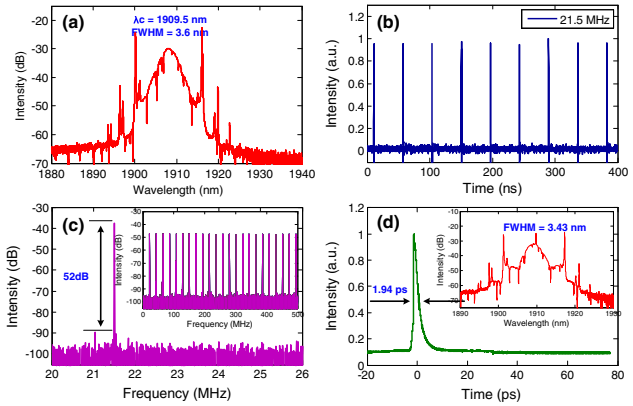

Fig. 3. Characteristics of fundamental mode-locked solitons; (a) optical spectrum; (b) pulse train; (c) RF spectrum, RBW = 1 kHz. Inset, span from 0 to 500 MHz; (d) autocorrelation trace at an amplified average power of ~60 mW. Inset, corresponding spectrum.

Fig. 3(a) match the water molecular absorption lines very well due to the spatial light propagation in the optical spectrum analyzer. The full-width half-maximum (FWHM) value of the output spectrum was measured to be 3.6 nm. Figure 3(b) plots the output pulse train with a pulse repetition rate of 21.5 MHz which corresponds to the inverse of the cavity round time. Benefitting from the high quality of the Bi_2Te_3 nanosheets and a relatively small loss of the TI-based SA, self-started mode-locking operation was observed. The soliton mode-locked THDFL had a high temporal stability and could work steady for 3 h every day during 1 week. The measured RF spectrum as shown in Fig. 3(c) had a signal-to-noise ratio higher than 50 dB. Figure 3(d) shows the measured autocorrelation trace with a temporal FWHM of 1.94 ps. By assuming a hyperbolic secant squared ($sech^2$) pulse profile, the output soliton width was only of ~1.26 ps. Figure 3(d), inset, shows that the spectral FWHM of the output soliton after amplification was 3.43 nm, which almost remained unchanged compared with the direct output solitons. The time–bandwith product (TBP) of the amplified soliton pulses is calculated to be 0.356, which is very close to the transform-limited value of a soliton pulse of 0.315.

When we increased the pump power to higher than 330 mW and kept the position of PC, the output of the THDFL behaved in accordance with the operation of soliton bunches. This phenomenon mainly originates from the fact that soliton pulse energy sustained in an abnormal laser cavity has a limited value [28,29]; when the intra-cavity gain increased the soliton pulses would be split and result in the multi-soliton operation. In the experiments, we found that the output split solitons were bunched together. The number of solitons in a single bunch could be continuously adjusted up to 15 by enhancing the pump with fixed PC position. Figure 4 plots typical soliton bunches output of the THDFL with different soliton numbers. As shown in Figs. 4(a) and 4(b), when the soliton number in a single bunch was less, these soliton pulses located very close to each other. By increasing the pump power, not only the soliton numbers in single bunch but also the distances between solitons were increased as shown in Figs. 4(c) and 4(d), which were typical characteristics of bunched soliton operation in mode-locked fiber lasers.

In the work, we also found pump hysteresis number in this mode-locked THDFL by comparing the effects of increasing and decreasing the pump power on the bunched soliton

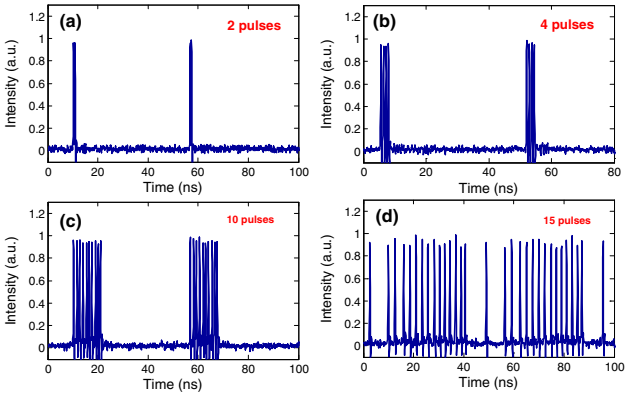

Fig. 4. Temporal characteristics of mode-locked THDFL with bunched soliton numbers as follows in a single bunch; (a) 2; (b) 4; (c) 10; (d) 15.

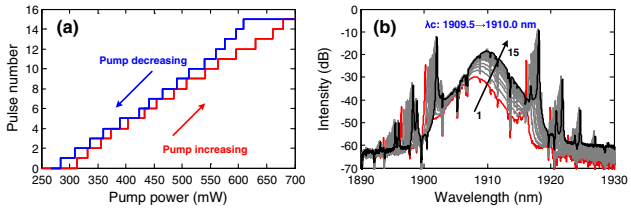

Fig. 5. Characteristics of soliton bunches; (a) hysteresis phenomenon of the bunched soliton number versus the pump power; (b) output spectra.

number as shown in Fig. 5(a). Due to the pump hysteresis phenomena, there were slight differences of pump power for the same bunched number; for example, the pump power required for the operation of 10-soliton bunch was 540.8–564.2 mW with increasing pump power, but it changed to 511.3–539.2 mW when we the pump power was decreased. Output spectra of these bunched solitons with different bunched numbers were also measured and are plotted in Fig. 5(b). It shows obviously that there were redshifts of both the spectral peaks and the Kelly sidebands. When the bunched number was increased from 1 to 15, the output central wavelength shifted from 1909.5 to 1910.0 nm.

Further, by adjusting the PC cautiously, the output soliton wavelength could also be tuned over a comparative broadband. Together with the adjusting of the 1570 nm pump power, harmonically mode-locked solitons with higher repetition rates could also appear in this mode-locked THDFL.

At this time, the soliton central wavelength was tuned to 1915 nm as shown in Fig. 6(d). With the increasing of the pump power, stable mode-locked soliton trains with repetition rate tuned from 21.5 to 215.04 MHz were observed, corresponding to the fundamentally mode-locked soliton train and the 10th-order harmonically mode-locked soliton train. Figures 6(a) and 6(b) show the fifth- and 10th-order harmonically mode-locked soliton trains, respectively. The evolution of the laser output power versus the 1570 nm pump power is plotted in Fig. 6(c). The experimentally observed three operation regions of the THDFL, namely, the self-lasing region, continuous-wave mode-locking region, and unstable region

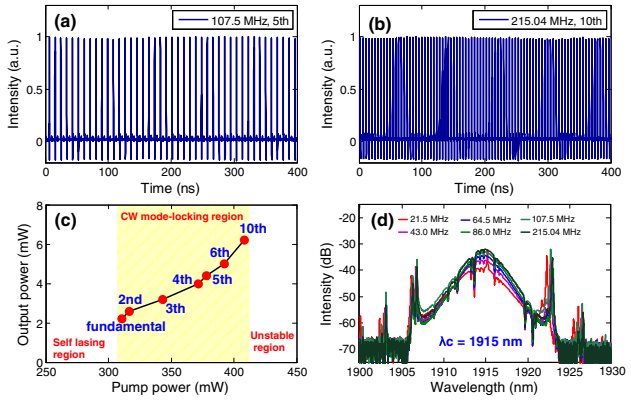

Fig. 6. Characteristics of harmonically mode-locked solitons; (a) soliton train for the fifth harmonic order; (b) soliton train for the 10th harmonic order; (c) evolutions of the output power and harmonic orders versus the pump power; (d) output spectra.

are depicted as well. It is important to mention that when the pump power was increased to higher than 413 mW, giant and restless soliton flows [29,30] were observed, and it was difficult to obtain stable mode-locked soliton trains anymore. Figure 6(d) shows the measured output soliton spectra. Distinct from the spectra of bunched solitons, there was no obvious redshifts of the output spectra when the harmonic mode-locking order of the THDFL was changed. Although the reason for this different spectral evolution is still unclear, we believe that the energy interaction among these bunched solitons might relate to it.

We have also verified whether the soliton mode-locking operation of the THDFL was dependent on the TI material. For this purpose, we replaced the TI-based SA with a similar piece of tapered SMF but without any Bi_2Te_3 nanosheet deposition. Although the PC was rotated and the pump power was adjusted on a very large scale, only continuous-wave self-lasing output could be observed. This comparative result showed that the soliton operation of the previously mentioned THDFL was indeed generated by TI Bi_2Te_3 nanosheets.

4. CONCLUSION

In conclusion, we have demonstrated diverse soliton mode-locking operations in a THDFL incorporated with a TI-based SA which was prepared by depositing Bi_2Te_3 nanosheets onto a piece of tapered fiber. By adjusting the pump power and the cavity polarization, fundamentally mode-locked soliton trains, soliton bunches, and harmonically mode-locked soliton trains at 1.9 μm region are realized. The output soliton pulse width is measured to be as short as 1.26 ps, with a TBP of 0.356 which is very close to the transform-limited value. The experimental results show that TI Bi_2Te_3 nanosheets could find applications in soliton mode-locked fiber lasers at 2 μm wavelength region like graphene and carbon nanotubes.

ACKNOWLEDGMENTS

The authors would like to thank Yu Chen and Chujun Zhao at Shenzhen University for the offer of TI Bi_2Te_3 materials. This work was supported by the State Key Program of National Natural Science of China (Grant Nos. 61235008, 61405254, 61340017, and 61435009), the Fundamental Researches Foundation of National University of Defense Technology (Grant No. GDJC13-04), and the Hunan Provincial Natural Science Foundation of China (Grant No. 14JJ3001).

REFERENCES

1. L. F. Mollenauer, R. H. Stolen, and J. P. Gordon, "Experimental observation of picosecond pulse narrowing and solitons in optical fibers," Phys. Rev. Lett. **45**, 1095–1098 (1980).
2. J. R. Taylor, *Optical Solitons: Theory and Experiment* (Cambridge University, 1992), Vol. **10**.
3. N. Q. Ngo, *Ultra-fast Fiber Lasers: Principles and Applications with MATLAB Models* (Taylor & Francis, 2011), Vol. **3**.
4. D. Y. Tang, B. Zhao, D. Y. Shen, C. Lu, W. S. Man, and H. Y. Tam, "Bound-soliton fiber laser," Phys. Rev. A **66**, 033806 (2002).
5. K. Kieu and M. Mansuripur, "Femtosecond laser pulse generation with a fiber taper embedded in carbon nanotube/polymer composite," Opt. Lett. **32**, 2242–2244 (2007).
6. F. Haxsen, D. Wandt, U. Morgner, J. Neumann, and D. Kracht, "Pulse characteristics of a passively mode-locked thulium fiber laser with positive and negative cavity dispersion," Opt. Express **18**, 18981–18988 (2010).
7. Y. F. Song, H. Zhang, D. Y. Tang, and D. Y. Shen, "Polarization rotation vector solitons in a graphene mode-locked fiber laser," Opt. Express **20**, 27283–27289 (2012).
8. D. Hsieh, D. Qian, L. Wray, Y. Xia, Y. S. Hor, R. J. Cava, and M. Z. Hasan, "A topological Dirac insulator in a quantum spin Hall phase," Nature **452**, 970–974 (2008).
9. Z. Luo, C. Liu, Y. Huang, D. Wu, J. Wu, H. Xu, Z. Cai, Z. Lin, L. Sun, and J. Weng, "Topological-insulator passively Q-switched double-clad fiber laser at 2 μm wavelength," IEEE J. Sel. Top. Quantum Electron. **20**, 0902708 (2014).
10. F. Bernard, H. Zhang, S. Gorza, and P. Emplit, "Towards mode-locked fiber laser using topological insulators," in *Nonlinear Photonics*, OSA Technical Digest, (OSA, 2012), paper NTh1A.5.
11. C. Zhao, H. Zhang, X. Qi, Y. Chen, Z. Wang, S. Wen, and D. Tang, "Ultra-short pulse generation by a topological insulator based saturable absorber," Appl. Phys. Lett. **101**, 211106 (2012).
12. Z. Luo, M. Liu, H. Liu, X. Zheng, A. Luo, C. Zhao, H. Zhang, S. Wen, and W. Xu, "2 GHz passively harmonic mode-locked fiber laser by a microfiber-based topological insulator saturable absorber," Opt. Lett. **38**, 5212–5215 (2013).
13. C. Chi, J. Lee, J. Koo, and J. H. Lee, "All-normal-dispersion dissipative-soliton fiber laser at 1.06 μm using a bulk-structured Bi_2Te_3 topological insulator-deposited side-polished fiber," Laser Phys. **24**, 105106 (2014).
14. C. Zhao, Y. Zou, Y. Chen, Z. Wang, S. Lu, H. Zhang, S. Wen, and D. Tang, "Wavelength-tunable picosecond soliton fiber laser with topological insulator: Bi_2Se_3 as a mode locker," Opt. Express **20**, 27888–27895 (2012).
15. J. Boguslawski, J. Sotor, G. Sobon, J. Tarka, J. Jagiello, W. Macherzynski, L. Lipinska, and K. M. Abramski, "Mode-locked Er-doped fiber laser based on liquid phase exfoliated Sb_2Te_3 topological insulator," Laser Phys. **24**, 105111 (2014).
16. J. Sotor, G. Sobon, W. Macherzynski, P. Paletko, K. Grodecki, and K. M. Abramski, "Mode-locking in Er-doped fiber laser based on mechanically exfoliated Sb_2Te_3 saturable absorber," Opt. Mater. Express **4**, 1–6 (2014).
17. H. Xia, H. Li, C. Lan, C. Li, X. Zhang, S. Zhang, and Y. Liu, "Ultrafast erbium-doped fiber laser mode-locked by a CVD-grown molybdenum disulfide (MoS_2) saturable absorber," Opt. Express **22**, 17341–17348 (2014).
18. R. Khazaeizhad, S. H. Kassani, H. Jeong, D.-I. Yeom, and K. Oh, "Mode-locking of Er-doped fiber laser using a multilayer MoS_2 thin film as a saturable absorber in both anomalous and normal dispersion regimes," Opt. Express **22**, 23732–23742 (2014).
19. J. Du, Q. Wang, G. Jiang, C. Xu, C. Zhao, Y. Xiang, Y. Chen, S. Wen, and H. Zhang, "Ytterbium-doped fiber laser passively mode locked by few-layer molybdenum disulfide (MoS_2) saturable absorber functioned with evanescent field interaction," Sci. Rep. **4**, 6346 (2014).
20. H. Zhang, S. B. Lu, J. Zheng, J. Du, S. C. Wen, D. Y. Tang, and K. P. Loh, "Molybdenum disulfide (MoS_2) as a broadband saturable absorber for ultra-fast photonics," Opt. Express **22**, 7249–7260 (2014).
21. M. Jung, J. Lee, J. Koo, J. Park, Y. Song, K. Lee, S. Lee, and J. H. Lee, "A femtosecond pulse fiber laser at 1935 nm using a bulk-structured Bi_2Te_3 topological insulator," Opt. Express **22**, 7865–7874 (2014).
22. G. Canat, W. Renard, E. Lucas, L. Lombard, J. Le Gouët, A. Durécu, P. Bourdon, S. Bordais, and Y. Jaouën, "Eyesafe high peak power pulsed fiber lasers limited by fiber nonlinearity," Opt. Fiber Technol. **20**, 678–687 (2014).
23. A. Pal, R. Sen, K. Bremer, S. Yao, E. Lewis, T. Sun, and K. T. V. Grattan, "'All-fiber' tunable laser in the 2 μm region, designed for CO_2 detection," Appl. Opt. **51**, 7011–7015 (2012).
24. M. Gebhardt, C. Gaida, P. Kadwani, A. Sincore, N. Gehlich, C. Jeon, L. Shah, and M. Richardson, "High peak-power mid-infrared $ZnGeP_2$ optical parametric oscillator pumped by a Tm:fiber master oscillator power amplifier system," Opt. Lett. **39**, 1212–1215 (2014).

25. W. Yang, B. Zhang, G. Xue, K. Yin, and J. Hou, "Thirteen watt all-fiber mid-infrared supercontinuum generation in a single mode ZBLAN fiber pumped by a 2 μm MOPA system," Opt. Lett. **39**, 1849–1852 (2014).
26. R. Thapa, D. Rhonehouse, D. Nguyen, Z. Yao, J. Zong, and A. Chavez-Pirson, "Ultra-wide mid-IR supercontinuum generation in W-type tellurite fiber pumped by 2 micron ultrashort laser," in *Frontiers in Optics 2012/Laser Science XXVIII*, OSA Technical Digest (Optical Society of America, 2012), paper FW4D.2.
27. C. W. Rudy, M. J. F. Digonnet, and R. L. Byer, "Advances in 2-μm Tm-doped mode-locked fiber lasers," Opt. Fiber Technol. **20**, 642–649 (2014).
28. Z. Luo, Q. Ning, H. Mo, H. Cui, J. Liu, L. Wu, A. Luo, and W. Xu, "Vector dissipative soliton resonance in a fiber laser," Opt. Express **21**, 10199–10204 (2013).
29. L. M. Zhao, D. Y. Tang, H. Zhang, and X. Wu, "Bunch of restless vector solitons in a fiber laser with SESAM," Opt. Express **17**, 8103–8108 (2009).
30. S. Chouli and P. Grelu, "Rains of solitons in a fiber laser," Opt. Express **17**, 11776–11781 (2009).